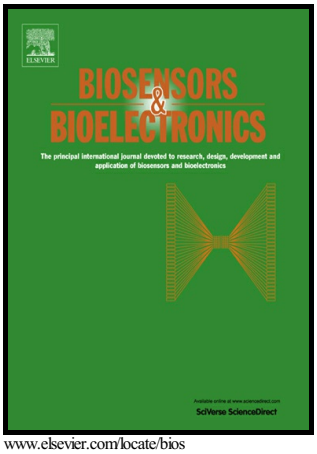


www.elsevier.com/locate/bios

# An enzyme-free surface plasmon resonance biosensor for real-time detecting microRNA based on allosteric effect of mismatched catalytic hairpin assembly

Jianbo Li, Pinhua Lei, Shijia Ding, Ye Zhang, Jianru Yang, Quan Cheng, Yurong Yan

PII: S0956-5663(15)30465-6
DOI: http://dx.doi.org/10.1016/j.bios.2015.09.069
Reference: BIOS8036

To appear in: *Biosensors and Bioelectronic*

Received date: 17 August 2015
Revised date: 28 September 2015
Accepted date: 29 September 2015

Cite this article as: Jianbo Li, Pinhua Lei, Shijia Ding, Ye Zhang, Jianru Yang, Quan Cheng and Yurong Yan, An enzyme-free surface plasmon resonance biosensor for real-time detecting microRNA based on allosteric effect o mismatched catalytic hairpin assembly, *Biosensors and Bioelectronic* http://dx.doi.org/10.1016/j.bios.2015.09.069

# An enzyme-free surface plasmon resonance biosensor for real-time detecting microRNA based on allosteric effect of mismatched catalytic hairpin assembly

Jianbo Li[a], Pinhua Lei[b], Shijia Ding[b], Ye Zhang[b], Jianru Yang[b], Quan Cheng[c], Yurong Yan[b,*]

[a] *Chongqing Engineering Research Center for Criminal Investigation Technology, Chongqing Medical University, Chongqing 400016, PR China*

[b] *Key Laboratory of Clinical Laboratory Diagnostics (Ministry of Education), College of Laboratory Medicine, Chongqing Medical University, Chongqing 400016, PR China*

[c] *Department of Chemistry, University of California, Riverside, California 92521, United States*

## Abstract

MicroRNAs (miRNAs) play significant regulatory roles in a variety of diseases and have been emerging as a group of promising biomarkers in cancer cells. Here, a novel and simple surface plasmon resonance (SPR) biosensor was developed for specific and highly sensitive detection of target miRNA employing the mismatched catalytic hairpin assembly (CHA) amplification coupling with programmable streptavidin aptamer (SA-aptamer). The presence of target miRNA triggered the allosteric effect of CHA amplification, which brought about the recycling of the target miRNA and produced large amounts of CHA products and activated SA-aptemers. Meanwhile, the plentiful CHA products could hybridize with the capture probes on the sensor chip, and the massive activated SA-aptamers could capture the streptavidin to achieve enhancement and output of the detection signal. Benefiting from the outstanding performance of the enzyme-free CHA amplification and non-label SPR biosensor, the established biosensor exhibited simplified process, high sensitivity and good selectivity. Under the optimal conditions, this designed strategy could detect target miRNA down to 1 pM with a dynamic range from 5 pM to 100 nM, and was successfully applied to the determination of target miRNA spiked into human total RNA samples. Thus, this SPR-based biosensor might become a potential alternative tool for miRNA detection in medical research and early clinical diagnosis.

**Keywords:** MicroRNAs; Catalytic hairpin assembly; Streptavidin aptamer; DNA-nanotechnology; Surface plasmon resonance

* Corresponding author. Tel: +86-23-68485688; Fax: +86-23-68485786.
E-mail address: yanyurong163@163.com.

## 1. Introduction

MicroRNAs (miRNAs) are a group of small (approximately 18-24 nucleotides), endogenous, and non-coding RNA molecules, which regulate the expression of target genes (Victor, 2004). MiRNAs play crucial roles in a variety of biological progresses such as cellular proliferation, differentiation, and apoptosis (Ventura and Jacks, 2009). Recent studies have found that aberrant expressions of miRNAs are implicated in many human diseases, including cancers (Lujambio et al., 2012), cardiovascular diseases (Deng et al., 2014), and neurological diseases (Eacker et al., 2009). It is revealed that miRNAs have emerged as a new group of promising biomarkers for early clinical diagnosis (Croce, 2009). Therefore, it is imperative to develop a simple and sensitive strategy for analyzing miRNA expression in clinical cases.

However, miRNAs have several unique properties, such as small sizes, low abundance, high sequence similarity, and liability to degradation, which increases the challenge for quantitative analysis (Duan et al., 2013). The traditional detection technologies for miRNAs are northern blotting (Válóczi et al., 2004), real-time PCR (Chen et al., 2005), and fluorescent microarray (Thomson et al., 2004). Although widely used, these methods have some drawbacks. For example, northern blotting is semi-quantitative and time-consuming (Varallyay et al., 2008). Real-time PCR is laborious, easy to generate false positive and requiring expensive equipment (Kroh et al., 2010). And fluorescent microarray requires extremely precise instrument and suffers from poor inaccuracy (Lagos-Quintana et al., 2011). Hence, it's important to establish novel analytical methods for miRNAs determination with good reliability and high sensitivity.

More recently, a range of researches have been implemented for miRNAs detection, such as colorimetry (Bi et al., 2013), fluorescence (Yang et al., 2012; Tu et al., 2013), chemiluminescence (Bi et al., 2011), electrochemical (Yu et al., 2014; Zhang et al., 2015), Raman spectroscopy (Abell et al.,

2012; Ye et al., 2014), and surface plasmon resonance (SPR) (Homola, 2008; Zhang et al., 2013; Šípová and Homola, 2013). Among these methods, surface plasmon resonance, as an optical biosensing technology, has attracted great attention owing to its unique advantages, such as label-free, sensitive, and real-time monitoring of biomolecular interactions (Homola, 2008).

In order to further improve the detection sensitivity and adaptability, various amplification strategies have been developed, e.g. rolling circle amplification (Liu et al., 2013; Deng et al., 2014), strand displacement assay (Shi et al., 2014; Zhou et al., 2014), enzymatic signal amplification (Cui et al., 2014; Wang et al., 2014), and nanomaterial-based assay (Li et al., 2014; Degliangeli et al., 2014). Although the detection sensitivity can be significantly improved, these methods have their weaknesses, including complex process, expensive reagents, poor reproducibility, and susceptible to the reaction conditions. Therefore, as an enzyme-free amplification method, catalytic hairpin assembly (CHA) has been developed from DNA nanotechnology and proven to be powerful in amplifying and transducing signals at the terminus of nucleic acid amplification reactions in recent years (Yin et al., 2008; Li et al., 2011;Liao et al., 2014). Due to its excellent property of signal amplification, CHA has been acquired extensive attention and can transduce analyte binding to a variety of detection modalities, such as colorimetric, fluorescent, and electrochemical signals (Chen et al., 2013; Jiang et al., 2013, 2014; Bhadra and Ellington, 2014). Thus, CHA can be utilized for the development of nonenzyme-based isothermal amplification strategies.

Herein, for the first time, a novel and simple strategy was developed for the miRNA detection by coupling the enzyme-free DNA nanotechnology with the non-label SPR biosensing platform. For the sake of decreasing the background signal and improving the analytical performance of CHA amplification strategy, mismatched base pairs of the breathing site in the hairpin-2 were introduced in this work. Moreover, we introduced the programmable streptavidin aptamer (SA-aptamer) (Zhuang et al., 2014) into the mismatched CHA amplification circuit, which could be activated by the allosteric effect of CHA reaction to enhance the detection signal and be flexible for the designation of CHA-based amplification strategy. The designed strategy provided excellent analytical performance in miRNA detection and possessed the potential to be an innovation of medical research and early clinical diagnosis.

## 2. Experiment section

2.1. Materials and Reagents

HPLC-purified DNA oligonucleotides were synthesized by Sangon Biotech (Shanghai, China). MiRNAs were obtained from TaKaRa Biotech (Dalian, China). Their sequences are listed in Table S1. All oligonucleotides were dissolved in TE buffer (10 mMTris-HCl, 1 mM EDTA, pH 8.0) and stored at -20 ℃. Total RNA extracted from human breast adenocarcinoma MCF-7 cells was obtained from Ambion (TX, USA). 6-Mercapto-1-hexanol (MCH) and streptavidin from Streptomyces avidinii were purchased from Sigma-Aldrich (St Louis, MO, USA). DL500DNA Marker and agarose were from TaKaRa Biotech (Dalian, China). GoldView was purchased from SBS Genetech (Beijing, China). Diethylpyrocarbonate (DEPC) was obtained from Solarbio (Beijing, China). All other reagents were of analytical grade. All aqueous solutions used in the experiments were prepared with Milli-Q water (≥ 18MΩ, Milli-Q, Millipore) and treated with DEPC and autoclaved to protect from RNase degradation. Hybridization buffer (TNaK buffer, pH 7.5) contained 20 mM Tris, 140 mM NaCl, and 5.0 mM KCl. Running buffer was 30 mM sodium phosphate containing 450 mM NaCl, 3 mM EDTA, and 0.25 % Triton×100 (pH 7.4).

2.2. Apparatus

The gel electrophoresis was carried out on the DYY-6C electrophoresis analyzer (Liuyi Instrument Company, China) and imaged on a Bio-Rad ChemDoc XRS (Bio-Rad, USA). The SPR Biacore X$^{TM}$ analytical system and the bare gold sensor chip were used (BIAcore AB, Uppsala, Sweden). The Biacore X$^{TM}$ displays results as a time course of resonance units (RU). All sensorgrams were displayed and evaluated using the BIA evaluation 4.1 software (Biacore, Sweden).

2.3. Preparation of probes

Hairpin probe 1 (H1) and hairpin probe 2 (H2) were designed based on the principle of the enzyme-free amplification system according to the sequence of miRNA-21. Before constructing the enzyme-free amplification system, both H1 and H2 were denatured at 95°C for 5 min and dropped 5 degrees per minute until cooling down to the room temperature. Then the probes were stored at 4°C for further use.

2.4. Preparation of SPR biosensor

The gold sensor chip was cleaned with fresh piranha solution (30% $H_2O_2$, 70% $H_2SO_4$) for 10 min to eliminate other substances, then washed thoroughly with deionized water several times, and

allowed to dry. The chip was docked into the Biacore X™ device. Until the baseline reached a steady state, 1 μM thiolated DNA probes in immobilization solution (1M $KH_2PO_4$, pH 3.8) were injected into the flow-cell and flowed through at a constant rate of 2 μL $min^{-1}$ for 30 min. After that, the chip was undocked and washed with deionized water, then blocked with 1 mM MCH solution for 4 h at room temperature in the dark. After washing with deionized water, the chip was left to dry and docked for further measurement.

The CHA amplification system consisted of hairpin probes (H1 and H2), TNaK buffer, RNAase inhibitor, and DEPC-treated water. The final reaction volume was 100 μL and the RNAase inhibitor reached a final concentration of 1 U $\mu L^{-1}$. After 1 h amplification reaction, the products were injected and hybridized with the capture probes immobilized on the sensor chip when the baseline was stable. Subsequently, the solution of 50 nM streptavidin in running buffer was injected and flowed through the flow-cell for 12 min. After that, the chip was washed with running buffer. All the hybridization experiments were carried out at a flow rate of 5 μL $min^{-1}$. After each detection process, 5 μL 50 mM NaOH was injected to remove the bound analytes on the gold film and washed with running buffer for the next detection.

2.5. Gel electrophoresis

To verify the feasibility of the CHA amplification system, the products and the sequences of the CHA reaction were analyzed by 8% native polyacrylamide gel electrophoresis (PAGE) in 1×TBE buffer (89 mM Tris−boric acid, 2 mM EDTA, pH 8.3) at a 110 V constant voltage for 60 min at 4°C before staining with Goldview (Saibaisheng, China). The gels were visualized via gel image system (Bio-Rad Laboratories, USA).

## 3. Results and discussion

3.1. Design of the SPR biosensor

An overview of the simple and rapid SPR detection of miRNA based on allosteric effect of catalyzed hairpin assembly and programmable streptavidin aptamer is illustrated in Scheme 1. Thiolated DNA probes, containing the sequence complementary to domain 2 and domain 5 of H1, are immobilized to the sensor surface by Au-S binding, and MCH is employed to block non-specific binding sites. H1 and H2 are primarily treated with gradient cooling processes for obtaining complete hairpin structures. In the presence of target miRNA, the stem of H1 will be unfolded. As a result, the

concealed sequence of H1's stem is exposed. Then with the interaction of H1 and H2, target miRNA is placed and released back to the next amplification circulation based on the toehold displacement mechanism. After that, the aptamer sequence of streptavidin is exposed with the formation of H1-H2 complexes. Subsequently, H1-H2 complexes are captured by the DNA probes on the sensor chip. Favorably, the streptavidin could clearly recognize the conformation of the SA-aptamer and strongly bind the aptamer to further amplify the response signal. A typical SPR sensorgram is depicted in Fig. 1. $\Delta RU_1$ shows the response of the hybridization of CHA products with capture probe. After that, the SA-aptamer is exposed by the allosteric effect of CHA circle and then combined with streptavidin, which means the response of $\Delta RU_2$. Therefore, the total response of each test is ($\Delta RU_1$+$\Delta RU_2$). After each test, the surface could be completely regenerated with the NaOH (50 mM) solution and make the dynamic curve back to the baseline for the next detection.

3.2. Design and validity of the CHA amplification circuit

The general principle of CHA was introduced in the seminal work by Pierce, Yin, and colleagues (Yin et al., 2008). Based on the principle of CHA, we designed a pair of hairpins (H1 and H2), shown in Scheme 1. The regions 1*, 2*, 3* in H1 were completely complementary to target miRNA. Region 2 and 5 were designed for hybridizing with the capture probe. In order to unfold H2, the regions 3, 4, 1 of H1 were designed complementary to H2. Improtantly, the programmable SA-aptamer was introduced as the partial regions (4 and 6) in H2. Owing to hybridization reaction at the stem region, the designed SA-aptamer was inactivated, and couldn't capture the subsequent streptavidin. With the aid of target miRNA, the allosteric effect of mismatched CHA circuit was initiated and the originally inactivated SA-aptamer sequence (region 4 and 6) was accordingly released by maintaining its single-stranded form, and thus was activated. After that it could improve the CHA strategy and enrich the mode of signal output. According to the above design and the sequence of miRNA-21, H1 and H2 were designed and the structures were drawn in Fig. 2A and Fig. 2B respectively. And the parameters of the hairpins were calculated by Oligo Analyzer 3.1. TNaK buffer (pH 7.5) contained 20 mM Tris, 140 mM NaCl, and 5.0 mM KCl was used when simulating the hairpins. The parameters are $\triangle G$ (gibbs free energy), $\triangle H$ (enthalpy change) and $\triangle S$ (entropy change) respectively. $\triangle H$ is used to dentify that the reaction is exothermic or endothermic. When the values of parameters are lower, the stem-loop structure designed by us is more stable and has rarely other secondary structure. These are

also helpful to CHA cycle to decrease the generation of large background signal.

To verify the validity of the CHA reaction, the products and the sequences of the CHA reaction were characterized by a 8% native polyacrylamide gel electrophoresis (PAGE). As shown in Fig. 2C, the base number of miRNA-21 (lane 1), H1 (lane2) and H2 (lane 3) derived from electrophoresis were consistent with our design. The target miRNA could successfully unfold H1 in lane 4, while H2 did not hybridize with the target miRNA in lane 5. In the absence of miRNA-21, only a few of H1 and H2 could potentially hybridize to form a H1:H2 duplex (land 6). However, with the target miRNA, the CHA reaction could be successfully carried out (land 7). And the signal-to-noise ratio was the comparison of the H1:H2 duplex between part b (lane 7) and part a (lane 6). To further verify the signal-to-noise ratio, the part a and b in Fig. 2C were analyzed with imageJ 1.48 software. The results in Fig. 2D indicated that the designed CHA strategy could be successfully conducted and possess a better signal-to-noise ratio. At the same time, the validation of the CHA amplification circuit has been performed with SPR sensorgram in Fig. S1.

3.3. Optimization of detection conditions

For the sake of obtaining excellent analytical performance, different experimental conditions were optimized (Fig. 3). Initially, the two hairpin substrates (H1 and H2) in a CHA circuit can potentially react non-specifically even in the absence of target miRNA, and this non-specific background degrades the signal-to-noise ratio. To reduce the prevalence of uncatalyzed strand exchange, we executed the mismatched CHA at the 3'-end of domain 2 in H2 (H2D2M2) (Zhang et al., 2015). H2 refers to the hairpin substrate, D2 refers to the domain, and M2 refers to the mismatched number (0, 1, 2, 3 and 4) (Table S1). As shown in Fig. 3A, the signal-to-noise ratio increased as the increasing mismatched number of H2D2M2 up to 2, but the signal-to-noise ratio decreased with the further increasing of mismatched number (Fig. 3A). Therefore, double mismatched number was chosen as the optimal mismatched number of H2D2M2. However, with the increasing of ratio of H1 to H2, the signal-to-noise ratio increased and then decreased at 1:1 (Fig. 3B), indicating that 1:1 was the optimal ratio of H1 to H2.

To further enhance the sensitivity, the incubating time of CHA and the concentration of SA were also optimized. The result of optimization of CHA incubating time was depicted in Fig. 3C. The signal-to-noise ratio ascended with the increase of incubating time. While the incubating time

extended to 60 min, the signal-to-noise ratio reached the peak and tended to decrease. Hence, 60 min was chosen as the optimal incubation time. The concentration of SA was also investigated from 10 nM to 100 nM (Fig. 3D). And the signal-to-noise ratio increased and then reached the maximum at 50 nM, suggesting that 50 nM was the optimal concentration of SA.

3.4. Analytical performance of miRNA detection

In order to evaluate the analytical performance of the designed biosensor, experiments were performed with different concentrations of target miRNA. Under optimal experimental conditions, the introduction of different concentrations of target miRNA to the sensor chip generated proportional increases in the response signal. The calibration plots showed a good linear relationship between the response signal and the logarithm of target miRNA concentrations in the range from 5 pM to 100 nM (Fig. 4A). The calibration curve for target miRNA could be simulated with a 4-parameter logistic equation: $f(c) = (A1 - A2)/(1 - (c/c_0)\,p) + A2$, while $f(c)$ is the SPR response signal and $c$ means the concentration of target miRNA. The calibration curve for detection of target miRNA (Fig. 4A) showed the values of (75.57±0.59) RU for $A1$, (514.40±6.12) RU for $A2$, (6.52±0.39) nM for $c_0$ and (0.81±0.01) for $p$. As recommended by the IUPAC (International Union of Pure and Applied Chemistry), the LOD is defined as the mean of the blank measures (64.24 RU) plus triple of its standard deviation (3 × 0.97= 2.91 RU) for higher than 99% confidence level (Loo et al., 2014). Based on this, the limits of detection (LODs) were calculated to be 1 pM. Considering the 100 μL detection volume per analysis, the smallest detectable absolute amount was less than 0.1 femtomoles. In the range of 500 pM to 50 nM, the response signal exhibited a very good linear relationship with the logarithm of target miRNA concentration (Fig. 4B), while the corresponding regression equation $Y(\Delta RU) = 154.94 + 174.24 \times lgC\,(nM)$ with the correlation coefficient of 0.9937. To further verify the merits of the designed strategy, the analytical properties were compared with those of other biosensors based on the CHA amplification in Table S2. It revealed that the mismatched CHA strategy proposed in this work possessed the feature of lower detection limit. In addition, the sensitivity of this biosensing strategy was compared to other nucleic acid detection methods by SPR biosensor technology in Table S3. Benefiting from enzyme-based amplification reactions or labeled amplifier, some works showed ultrawide range and ultrasensitive detection for nucleic acid targets, while others just hold general analytical performances. Moreover, the current strategy not only had wider linear range and lower

limit of detection, but also held easy and rapid progress due to the non-label and enzyme-free design. It suggested that the proposed method could be applied to rapid and highly sensitive detection of miRNA.

3.5 Specificity, reproducibility and reusability of the strategy

The specificity of the established SPR method was evaluated by detecting five different miRNA sequences, including the perfect complementary target miRNA, single-base mismatch target (SM), double-base mismatch target (DM), non-complementary sequence (NC), and miR-222 at the same concentration of 25 nM. As shown in Fig. 5A, the response signals of DM, NC and miR-222 were similar to that of blank. However, it was clear that there was a remarkable increase in the response signal when target miRNA existed. And the response of target miRNA was about 2.5 times as that of SM (Fig. 5B). In addition, the reproducibility of the designed method was further investigated. Five replicate measurements of miRNA-21 at the concentrations of 0.1 nM and 25 nM showed the variation coefficients of 1.0% and 1.1%, respectively. In order to explain the reusability of the biosensor, repeated regenerations were carried out on the same chip. The sensor chip could be regenerated 100 times while the SPR response only decreased less than 10 %.

3.6 Recovery test

To verify the potential application of the proposed method in real sample analysis, we performed the recovery test using MCF-7 total RNA as an example. The total RNA sample was diluted to 400 ng $\mu L^{-1}$ with DEPC-treated water, and 2.5μL total RNA sample diluted to 100 μL with TNaK buffer (1μg in total) was used for measurement. According to the calibration curve (Fig. 4A), the amount of miRNA-21 in1μg total RNA sample was estimated to be 4 fmol (RSD = 0.2%, n= 5). To further evaluate its performance in real sample analysis, different amounts of miRNA-21 were spiked into 1 μg total RNA for the assay, and the results showed the recovery of 103.2% -115.6% (Table. S4 and Figure. S2), demonstrating that the designed strategy could be a potential tool for analyzing miRNA in real samples.

## 4. Conclusion

In summary, we have successfully developed a simple and novel SPR biosensing strategy for miRNA detection using mismatched CHA amplification system and programmable SA-aptamer. The enzyme-free CHA amplification overcame the disadvantages of traditional enzyme-based

amplification and obtained satisfactory results in the decrease of background signal of CHA system with the introduction of mismatched base pairs of the breathing site in hairpin-2. Moreover, the caged programmable SA-aptamer in hairpin probe 2 could be activated after allosteric of the CHA circuit. In addition, the activated SA-aptamer was utilized as a signal amplifier in this developed strategy and possessed the potential to the innovation of many flexible strategies. Due to the excellent analytical performance, the designed strategy could detect target miRNA as low as 1 pM with a wide linear range and obtain good performance in real sample analysis with simple process and good repeatability. Therefore, this developed biosensor possesses potentials to be a versatile strategy for miRNA detection in medical research and early clinical diagnosis.

**Acknowledgements**

This work was funded by the National Natural Science Foundation of China (81371904), the Natural Science Foundation Project of CQ (CSTC2013jjB10019), Application Development Plan Project of Chongqing (cstc2014yykfB10003), and the Science and Technology Plan Project of Yuzhong District of Chongqing (20120212).

**References**

Abell, J.L., Garren, J.M., Driskell, J.D., Tripp, R.A., Zhao, Y.P., 2012. J. Am. Chem. Soc. 134, 12889-12892.

Bhadra, S., Ellington, A.D., 2014. Nucleic Acids Res. 42, e58.

Bi, S., Cui, Y.Y., Li, L., 2013. Anal. Chim. Acta. 760, 69-74.

Bi, S., Zhang, J., Hao, S., Ding, C., Zhang, S., 2011. Anal. Chem. 83, 3696-3702.

Chen, C., Ridzon, D.A., Broomer, A.J., Zhou, Z., Lee, D.H., Nguyen, J.T., Barbisin, M., Xu, N.L., Mahuvakar, V.R., Andersen, M.R., Lao, K.Q., Livak, K.J., Guegler, K.J., 2005. Nucleic Acids Res. 33, e179.

Chen, X., Briggs, N., McLain, J.R., Ellington, A.D., 2013. PANS 110, 5386-5391.

Croce, C.M., 2009. Nat. Rev. Genet. 10, 704-714.

Cui, L., Zhu, Z., Lin, N.H., Zhang, H.M., Guan, Z.C., Yang, C.Y., 2014. Chem. Commun. 50, 1576-1578.

Degliangeli, F., Kshirsagar, P., Brunetti, V., Pompa, P.P., Fiammengo, R., 2014. J. Am. Chem. Soc. 136, 2264-2267.

Deng, R.J., Tang, L.H., Tian, Q.Q., Wang, Y., Lin, L., Li, J.H., 2014. Angew. Chem. Int. Ed. 53, 2389-2393.

Duan, R.X., Zuo, X.L., Wang, S.T., Quan, X.Y., Chen, D.L., Chen, Z.F., Jiang, L., Fan, C.H., Xia, F., 2013. J. Am. Chem. Soc. 135, 4604-4607.

Eacker, S.M., Dawson, T.M., Dawson, V.L., 2009. Nat. Rev. Neurosci.10, 837-841.

Homola, J., 2008. Chem. Rev. 108, 462-493.

Jiang, Y.S., Li, B.L., Milligan, J.N., Bhadra, S., Ellington, A.D., 2013. J. Am. Chem. Soc. 135, 7430-7433.

Jiang, Y.S., Bhadra, S., Li, B.L., Ellington, A.D., 2014. Angew. Chem. Int. Ed. 126, 1876-1879.

Kroh, E.M., Parkin, R.K., Mitchell, P.S., Tewari, M., 2010. Methods 50, 298-301.

Lagos-Quintana, M., Rauhut, R., Lendeckel, W., Tuschl, T., 2011. Science 294, 853-858.

Li, B.L., Ellington, A.D., Chen, X., 2011. Nucleic Acids Res. 39, e110.

Li, F.Y., Peng, J., Wang, J.J., Tang, H., Tan, L., Xie, Q.J., Yao, S.Z., 2014. Biosens. Bioelectron. 54, 158-164.

Liao, Y.H., Huang, R., Ma, Z.K., Wu, Y.X., Zhou, X.M., Xing, D., 2014. Anal. Chem. 86, 4596-4604.

Liu, H.Y., Li, L., Duan, L.L., Wang, X., Xie, Y.X., Tong, L.L., Wang, Q., Tang, B., 2013. Anal. Chem. 85, 7941-7947.

Loo, F.C., Ng, S.P., Wu, C.L., Kong, S.K., 2014. Sensor. Actuat B-Chem. 198, 416-423.

Lujambio, A., Lowe, S.W., 2012. Nature 482, 347-355.

Shi, C., Liu, Q., Ma, C., Zhong, W., 2014. Anal. Chem. 86, 336-339.

Šípová, H., Homola, J., 2013. Anal. Chim. Acta 773, 9-23.

Thomson, J.M., Parker, J., Perou, C.M., Hammond, S.M., 2004. Nat. Methods 1, 47-53.

Tu, Y.Q., Li, W., Wu, P., Zhang, H., Cai, C.X., 2013. Anal. Chem. 85, 2536-2542.

Válóczi, A., Hornyik, C., Varga, N., Burgyán, J., Kauppinen, S., Havelda, Z., 2004. Nucleic Acids Res. 32, e175.

Varallyay, E., Burgyan, J., Havelda, Z., 2008. Nat. Protoc. 3, 190-196.

Ventura, A., Jacks, T., 2009. Cell 136, 586-591.

Victor, A., 2004. Nature 431, 350-355.

Wang, M., Fu, Z.L., Li, B.C., Zhou, Y.L., Yin, H.S., Ai, S.Y., 2014. Anal. Chem. 86, 5606-5610.

Yang, L., Liu, C., Ren, W., Li, Z., 2012. ACS Appl. Mater. Interfaces 4, 6450-6453.

Ye, L.P., Hu, J., Liang, L., Zhang, C.Y., 2014. Chem. Commun. 50, 11883-11886.

Yin, P., Choi, H.M., Calvert, C.R., and Pierce, N.A., 2008. Nature 451, 318-322.

Yu, Y.Y., Chen, Z.G., Shi, L.J., Yang, F., Pan, J.B., Zhang, B.B., Sun, D.P., 2014. Anal. Chem. 86, 8200-8205.

Zhang, D.C., Yan, Y.R., Cheng, W., Zhang, W., Li, Y.H., Ju, H.X., Ding, S.J., 2013. Microchim. Acta 180, 397-403.

Zhang, Y., Yan, Y.R., Chen, W.H., Cheng, W., Li, S.Q., Ding, X.J., Li, D.D., Wang, H., Ju, H.X., Ding, S.J., 2015. Biosens. Bioelectron. 68, 343-349.

Zhou, D.M., Du, W.F., Xi, Q., Ge, J., Jiang, J.H., 2014. Anal. Chem. 86, 6763-6767.

Zhuang, J.Y., Tang, D.P., Lai, W.Q., Chen, G.N., Yang, H.H., 2014. Anal. Chem. 86, 8400-8407.

**Figure captions**

**Scheme 1** Schematic representation of miRNA SPR biosensor based on mismatched catalytic hairpin assembly amplification coupling with streptavidin aptamer.

**Fig. 1** Typical sensorgram of CHA products hybridized with capture probe and streptavidin signal amplification.

**Fig. 2** (A) Ideal structure and parameters of hairpin probe 1, (B) ideal structure and parameters of hairpin probe 2, (C) electrophoresis of CHA amplification products, the final concentration of miRNA, H1, H2 is 1 uM in every lane, and the incubating time is 1 hour. (D) Validation of part a and b in Fig. 2C (derived from ImageJ 1.48 sortware).

**Fig. 3** Optimizations of experimental parameters: (A) evaluation of the effect of mismatched base pair number in H2, (B) evaluation of the effect of the ratio of H1 to H2, (C) evaluation of the effect of the incubating time of CHA reaction, and (D) evaluation of the effect of the concentration of streptavidin. All the parameters were evaluated on the signal to noise ratio.

**Fig. 4** (A) The calibration curve of △RU versus target miRNA at 0, 0.001, 0.005, 0.01, 0.025, 0.05, 0.1, 0.25, 0.5, 1.0, 2.5, 5, 10, 25, 50, and 100 nM. (B) SPR sensorgrams for detection of target miRNA at 50, 25,10,5, 2.5, 1.0, and 0.5 nM (from a to g) and the

inset shows a good relationship between signal response and target miRNA from 0.5 nM to 50 nM.

**Fig. 5** (A) SPR sensorgrams and (B) SPR signal response respectively corresponding to 25 nM of target miRNA (a), single-base-mismatched oligonucleotides (b), two-base-mismatched oligonucleotides (c), non-complementary oligonucleotides (d), mir-222 (e) and blank (f).

## Highlights

A novel and enzyme-free SPR biosensing has been developed for miRNA detection based on allosterci effect of mismatched catalytic hairpin assembly and programmable streptavidin aptamer.

The designed mismatched CHA amplification system could overcome the disadvantages of enzyme-based amplification and greatly improve the analytical performance of miRNA detection with satisfied signal to noise ratio.

The programmable streptavidin aptamer has been introduced into the CHA amplification system, which could improve the performance of CHA reaction and would become versatile ideas in other biosensors.

The developed SPR biosensor displays high sensitivity, good specificity and repeatability for miRNA detection and successfully applied to detect target miRNA in human total RNA sample.